

# Changes in silicate utilisation and upwelling intensity off Peru since the Last Glacial Maximum – insights from silicon and neodymium isotopes

C. Ehlert\*, P. Grasse, M. Frank

GEOMAR Helmholtz Centre for Ocean Research Kiel, Germany

---

Article history:

Received 6 November 2012

Received in revised form

11 April 2013

Accepted 19 April 2013

Available online

---

Keywords:

Silicate utilisation

Silicon isotopes

Diatoms

Neodymium isotopes

Peruvian upwelling

Upwelling intensity

ENSO intensity

---

We combine the stable silicon isotope composition ( $\delta^{30}\text{Si}$ ) of diatoms and the radiogenic neodymium isotope compositions ( $\varepsilon_{\text{Nd}}$ ) of past seawater extracted from the authigenic fraction of the sediments (Mn–Fe coatings of particles and benthic foraminifers), as well as the radiogenic isotope compositions (Nd, Sr) of the detrital material itself to reconstruct silicic acid utilisation, water mass mixing, and upwelling intensity from the same marine sediments in the Peruvian upwelling region during the past 20,000 years. Additionally, the sedimentary signals were compared to the water column isotope compositions.

Along the Peruvian shelf, the dissolved  $\varepsilon_{\text{Nd}}$

---

### 1.1. Nutrient cycling, utilisation and silicon isotopes

In the Peruvian upwelling system primary productivity is dominated by diatoms (Estrada and Blasco, 1985; Abrantes et al., 2007) which build their opaline frustules from dissolved silicic acid ( $\text{Si(OH)}_4$ ) (Trégouer et al., 1995). The nutrients feeding the productivity are mainly supplied via upwelling of the southward flowing subsurface waters of the Peru–

masses acquire their Nd isotope composition (expressed as  $\varepsilon_{\text{Nd}}$ , which corresponds to the measured  $^{143}\text{Nd}/^{144}\text{Nd}$ , normalised to the Chondritic Uniform Reservoir CHUR (0.512638), multiplied by 10,000) in their source regions through weathering of continental rocks with distinct isotopic signatures supplied to the oceans via rivers, eolian inputs or through shelf exchange processes (e.g. Frank, 2002; Lacan and Jeandel, 2005). In the EEP three main endmembers dominate the Nd isotope signal. Water masses of Southern Ocean origin have less radiogenic signatures between -5 and -9 (Piepgras and Wasserburg, 1982;



(n =

Table 3

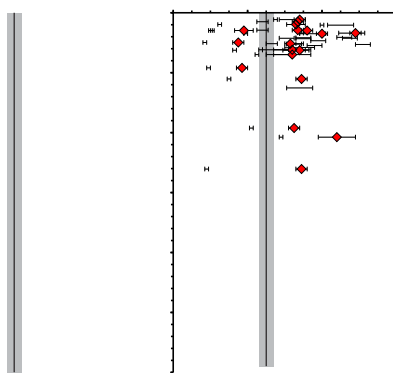
Downcore records of core SO147-106KL for  $\delta^{30}\text{Si}$  ( $\text{bSiO}_2$  and picked diatoms),  $^{87}\text{Sr}/^{86}\text{Sr}$ ,  $^{143}\text{Nd}/^{144}\text{Nd}$  and  $\varepsilon_{\text{Nd}}$  (Fe

---



radiogenic (mean  $\varepsilon_{\text{Nd}} = -4.3 \pm 1.8$ ,  $2\sigma_{\text{sem}}$ ) than the water. In deep waters below 1000 m the  $\varepsilon_{\text{Nd}}$  signature of seawater and detrital fraction have similar values around  $-4$ , whereas the authigenic fraction remains more radiogenic at values around  $-0.8$  (Fig. 3e).

Overall the latitudinal variations of the detrital signal and the dissolved  $\varepsilon_{\text{Nd}}$  in the surface waters generally covary (Fig. 2b). Within the subsurface waters, seawater and authigenic  $\varepsilon_{\text{Nd}}$  are overall similar to each other with rather homogenous  $\varepsilon_{\text{Nd}}$  values



between  $-1.4$  and  $-1.9$  all along the shelf between the equator and  $16^{\circ}\text{S}$  (Fig. 3f). In the intermediate waters, the dissolved  $\epsilon_{\text{Nd}}$  again shows no clear trend, whereas the authigenic (both coatings and benthic foraminifera) overall decrease from North to South whereas the detrital sediment fraction shows pronouncedly unradiogenic values at  $4\text{--}8^{\circ}\text{S}$  and near  $16^{\circ}\text{S}$  (Fig. 3g).

The  $\epsilon_{\text{Nd}}$  signature of the Fe–Mn coatings and the benthic for-

ranged between 0.70620 and 0.70849 and shows a variability closely following that of the  $\varepsilon_{\text{Nd}}$

and show only a slight trend towards less radiogenic values with depth (Fig. 3c–e) and with latitude towards the south (Fig. 3f–h). In general, the water mass Nd isotope signatures and mixtures in the EEP are dominated by three main endmembers: the Southern Ocean characterised by less radiogenic signatures between –5 and –9 (Piepgras and Wasserburg, 1982; Stichel et al., 2012) and the northern and central Pacific with more radiogenic  $\epsilon_{\text{Nd}}$  signatures between –5 and –2 (Piepgras and Jacobsen, 1988; Amakawa et al., 2009). Along the continental margin the water column profiles show comparably radiogenic  $\epsilon_{\text{Nd}}$  values around –1.9 within the

intensity (Brink et al., 1983), primary biological productivity (Fiedler, 2002; Pennington et al., 2006) and the rainfall regime (Bendix, 2000; Baker et al., 2001). Paleo records suggest persistent ENSO variability at millennial timescales throughout the Last Glacial–interglacial cycle, but overall weaker El Niño intensity (lower frequency and amplitude of major events) seems to have prevailed during the latest Pleistocene and the first half of the Holocene, with respect to the late Holocene (Rodbell et al., 1999; Tudhope et al., 2001). However, this interpretation is not consistent in all records. For example, carotenoid pigment data by Rein et al. (2005) reveal high primary productivity during the early and late Holocene (Fig. 5), which has been related to enhanced upwelling and nutrient supply due to higher La Niña intensity. In contrast, alkenone-derived SSTs (Rein et al., 2005) indicate that highest temperatures/weakest upwelling and therefore weakest nutrient re-supply from subsurface waters also occurred during these periods of time (Fig. 5). These contradictory results may be a consequence of the sedimentary integration of different archives recording the opposing ENSO states. The combined proxy records of  $\epsilon_{\text{Nd}}$ , bSiO<sub>2</sub> MAR and  $\delta^{30}\text{Si}_{\text{opal}}$  in our study now provide a unique window into past ENSO variability and document fundamental changes in upwelling and nutrient supply conditions during the past 20 ka. El Niño- and La Niña-like conditions alternating on seasonal and interannual timescales left their signal in the sedimentary record.

#### 4.2.1. Past changes in circulation and upwelling intensity

The  $\epsilon_{\text{Nd},\text{coating}}$  record does not indicate any major changes water

(Reynolds et al., 2008; Pichevin et al., 2012). At complete utilisation the  $\delta^{30}\text{Si}_{\text{opal}}$  would be equal to the dissolved  $\delta^{30}\text{Si}_{\text{Si(OH)}_4}$  of the source water ( $= +1.4\text{\textperthousand}$ ) (Fig. 7). This value is in good agreement with actual measurements of  $\delta^{30}\text{Si}_{\text{Si(OH)}_4}$  from the present-day upwelling subsurface source waters ( $\delta^{30}\text{Si}_{\text{Si(OH)}_4} = +1.5\text{\textperthousand}$ , Ehlert et al., 2012) indicating that the highest  $\delta^{30}\text{Si}_{\text{opal}}$  values during the early and late Holocene reflect near-complete  $\text{Si(OH)}_4$  utilisation.

Present day surface waters in the area of the core location (between 5°S and 15°S) have relatively low  $\delta^{30}\text{Si}_{\text{Si(OH)}_4}$  between  $+1.7\text{\textperthousand}$  and  $2\text{\textperthousand}$ , because the re-supply of  $\text{Si(OH)}_4$  via upwelling is relatively constant, and the fractionation due to limitation is low. The degree

euphotic zone along the Peruvian shelf was reduced (Huyer et al., 1987). This has led to decreased primary productivity (Feldman et al., 1984; Chavez, 2005), less oxygen consumption through decay of organic matter, which in turn has led to decreased Fe and P supply from the underlying sediments. Under Fe-limited conditions, however, diatoms reveal a higher Si:N uptake ratio (they are more strongly silicified, but also more likely Si(OH)<sub>4</sub> limited) (Takeda, 1998; Hutchins et al., 2002; Baines et al., 2010) which leads to an increased export of Si (via bSiO<sub>2</sub>) relative to N and which affects the interpretation of the bSiO<sub>2</sub> record in tei4b3L05..8(of)-449.21.31946203159TD[(leadsnutri)-3.5(Thi4(ut)]Ts)-4453.5(Th(C-28eq.1(oducti)12.145.83aheede.42shelfL.9(6(has7.glacial-2(e259(op86.3(alod)bur3al-2(e252(rat.alod)s.2(e74.-1.3159TD[(tions,38.2557(EEP.2550c]TJ0.0

Similar to our observations of bSiO<sub>2</sub> MAR and Si(OH)<sub>4</sub> utilisation, and in contrast to the results by Rein et al. (2005), Carré et al. (2005) found that SSTs in southern Peru were about 3 °C colder during the early Holocene compared to the late Holocene, indicating stronger upwelling conditions during that time. Vargas et al. (2006) on the other hand found several debris flows in southernmost Peru dated for the time period 12.9 to 8.4 ka BP, which were interpreted to be associated with intense rainfall episodes that must have occurred during non-El Niño conditions, concomitant with intensified coastal upwelling. These different findings indicate a high variability of the system alternating between El Niño and La Niña conditions during the early Holocene with warm SSTs, variable primary bioproductivity and strong El Niño related flooding events.

#### 4.2.5. The late Holocene off Peru (2.5–1 ka)

All applied proxies document a highly variable environment along the Peruvian shelf during the late Holocene. The bSiO<sub>2</sub> MAR, similar to the carotenoid pigment fluxes, increased strongly around 2 ka resulting in high sedimentary bSiO<sub>2</sub> contents up to 20–30 wt%. This was accompanied by the highest  $\delta^{30}\text{Si}_{\text{opal}}$  signatures of up to +1.4‰. Calculating surface water  $\delta^{30}\text{Si}_{\text{Si(OH)}_4}$  values of +2.5‰ results in estimates for Si(OH)<sub>4</sub> utilisation between 90 and 100% (Fig. 7), which represents the highest level during the past 20 ka. A 90% utilisation can today only be found in those areas of weaker upwelling and lower nutrient re-supply to the surface water (Ehlert et al., 2012). During the late Holocene the  $\varepsilon_{\text{Nd}_{\text{detritus}}}$  signal showed the largest variability within the past 20 ka. It was characterised by a pronounced decrease from –1.5 to values around –4.5 between 4 and 1.2 ka. The surface sediment in that area is also characterised by less radiogenic  $\varepsilon_{\text{Nd}_{\text{detritus}}}$  values around –3.2 compared to the areas further north. In particular, the signatures of the last 2 ka were very different from the rest of the record. The highly unradiogenic  $\varepsilon_{\text{Nd}_{\text{detritus}}}$  and radiogenic  $^{87}\text{Sr}/^{86}\text{Sr}_{\text{detritus}}$  would be consistent with enhanced dust input from the Atacama Desert in southern Peru and northern Chile (Fig. 6) (Molina-Cruz, 1977). However, climatic reconstructions indicate a general southward shift in the mean position of the Intertropical Convergence Zone during the Holocene (Haug et al., 2001), which caused higher precipitation in the Peruvian region (Bendix, 2000; Baker et al., 2001) and thus a more locally dominated input of material. At the same time high bSiO<sub>2</sub> content and high Si(OH)<sub>4</sub> utilisation required stronger upwelling of nutrient-rich subsurface waters, which usually occurs during La Niña-like conditions. The observed timing and high variability in our record confirms that, although the early Holocene record shows some characteristics of high ENSO intensity, very strong ENSO patterns only operated during the second half of the Holocene and that the onset of modern ENSO conditions did not occur prior to 5.5 ka BP, with increased frequency of major events only during recent times (Loubere et al., 2003; Carré et al., 2005; Vargas et al., 2006; Toth et al., 2012). It was only during the latest Holocene of the past 2–3 ka that the Peruvian shelf area experienced persistently more moderate productivity conditions, with shorter periods of increased productivity (Agnihotri et al., 2008).

## 5. Conclusions

Surface sediments along the Peruvian margin were analysed for their radiogenic Nd isotope composition, and compared to water column measurements from the same area. In general, all phases (seawater, Fe–Mn coatings, benthic foraminifers and detrital material) display a trend from more radiogenic values in the North towards less radiogenic values in the South, which is in good agreement with the distribution of the signatures of the outcropping rocks of the Andean hinterland. Authigenic  $\varepsilon_{\text{Nd}}$  signatures are mostly significantly more radiogenic than the seawater or detrital



western North Atlantic since the Last Glacial Maximum from Blake Ridge sediments. *Earth and Planetary Science Letters* 266 (1–2), 61–77. <http://dx.doi.org/10.1016/j.epsl.2007.10.037>.

Stumpf, R., Frank, M., Schönfeld, J., Haley, B.A., 2011. Climatically driven changes